GENOMICS
In press
2000

Title: Physical interactions among human checkpoint control proteins HUS 1p, RAD1p and RAD9p, and implications for the regulation of cell cycle progression.

Authors: Haiying Hang and Howard B. Lieberman

Address: Center for Radiological Research, Columbia University, 630 West 168" St., New York, NY 10032

Running title: HUS1p, RAD1p and RAD9p protein interactions

Accession no.: AF110393 (*HUS1* cDNA)

Corresponding author: Howard B. Lieberman

Center for Radiological Research

Columbia University

630 West 168th St.

New York, NY 10032.

Tel. #/FAX #: (212) 3059241

E-mail: lieberman@cuccfa.ccc.columbia.edu

ABSTRACT

Schizosaccharomyces pombe husl promotes radioresistance and hydroxyurea resistance, as well as S and G2 phase checkpoint control. We isolated a human cDNA homologous to ***husl,*** called *HUS1*. The major focus of this report is on a detailed analysis of the physical interactions of the *HUS1*-encoded protein, and two other checkpoint control proteins, RADlp and RAD9p, implicated in the cellular response to DNA damage. We found that HUS lp interacts with itself and the N-terminal region of RADlp. In contrast, the C-terminal portion of the checkpoint protein RAD9p is essential for interacting with HUS1p and the C-terminal region of RADlp. Since the N-terminal portion of RAD9p was previously demonstrated to participate in apoptosis, this protein likely has at least two functional domains, one that regulates programmed cell death and the other cell cycle checkpoint control. Truncated versions of HUS lp are unable to bind RADlp, RAD9p or another HUS 1 p molecule. RAD 1 p-RAD 1 p and RAD9p-RAD9p interactions can be demonstrated by coimmunoprecipitation, but not by two-hybrid analysis, suggesting that the proteins associate as part of a complex but do not interact directly. Northern blot analysis indicates that *HUS1* is expressed in different tissues, but the mRNA is most predominant in testis where high levels of *RAD1* and *RAD9* message have been detected. These studies suggest that HUS lp, RAD9p and RAD1p form a complex in human cells, and may function in a meiotic checkpoint in addition to the cell cycle delays induced by incomplete DNA replication or DNA damage.

INTRODUCTION

Cells replicate their genomic DNA and divide in a specific temporal order within the cell cycle. Nuclear division with incompletely replicated or damaged genomic DNA can lead to cell death or the production of genetically compromised daughter cells with a predilection for the development of cancer (Hartwell and Kastan, 1994; Nojima, 1997). The progression of cell cycle events and their coordination with the maintenance of genomic DNA integrity are regulated by mechanisms termed checkpoints (Hartwell and Weinert, 1989). In the fission yeast *Schizosaccharomyces pombe,* six checkpoint genes (*hus1, radl, rad3, rad9, rad17* and *rad26) are* essential for S/M and G2/M checkpoint controls, as well as for promoting resistance to the DNA replication inhibitor hydroxyurea or radiation (for review see Griffiths and Carr, 1997). With the exception of *rad26,* human homologues of these yeast genes have been cloned (i.e., *HUS1*, *RAD1, ATR, RAD9* and *RAD17*; Kostrub et al., 1998; Parker *et al.,* 1998a, b; Freire *et al.,* 1998; Udell *et al.,* 1998; Dean *et al.,* 1998; Cimprich *et* al., 1996; Lieberman *et al.,* 1996), and there is mounting evidence that they too play a role in cell cycle checkpoint control. For example, overexpression of *RAD1*, *RAD9* or *RAD17* can partially complement the radiosensitivity, hydroxyurea sensitivity and/or accompanying checkpoint control defects of corresponding mutant *S. pombe* cells (Lieberman *et al.,* 1996; Udell *et al., 1998;* Li *et al., 1999). ATR,* the human homologue of *rad3*, regulates G1, S and G2 checkpoint controls in response to irradiation, and also promotes radioresistance in human cells (Cliby *et al.,* 1998; Wright *et al.,* 1998; Smith *et al.,* 1998). Overexpression of a catalytically inactive form of *ATR* in human fibroblasts inhibits the phosphorylation of Ser-15 in p53 after exposure to gamma-rays or UV light, suggesting that p53 is

a target for phosphorylation by ATR in cells with DNA damage (Tibbetts et al., 1999). **When** *RAD1* 7 is overexpressed in human fibrosarcoma cells p53 becomes activated and cells accumulate in G1 (Li et al., 1999). Furthermore, when *MRAD17*, the mouse version of *RAD17*, contains mutations in its putative DNA binding domain and is overexpressed in human cells methyl methane sulfonate can no longer efficiently induce a transient delay in the G2 phase of the cell cycle (Bao *et al.,* 1998). The high degree of structural conservation between the related yeast and mammalian versions of the encoded proteins, as well as the cross-species complementation and similar activities observed suggest that these genes and their functions in checkpoint control have been preserved throughout evolution.

Two versions of *HUS1*, one containing an 843 bp open reading frame alone and a second that is a 2.1 kb full-length cDNA, have been reported independently by Kostrub *et al.* (1998) and Dean *et* al. (1998), respectively. In this study, we describe a cDNA (accession no. AF110393) that is similar to the one reported by Dean et al. (1998) but for a few bps, and encodes the same amino acids. HUS lp was found by several other investigators to interact with RADlp and RAD9p, using coimmunoprecipitation and two-hybrid strategies (Volkmer and Karnitz, 1999; St. Onge et al., 1999). These interactions reflect the previous finding that *S. pombe* hus lp and radlp proteins interact in a rad9p-dependent manner (Kostrub *et al.,* 1998). We show here that HUSlp can also physically interact with at least one other HUS lp molecule. Furthermore, we found that the amino terminal region of RADlp and the carboxyl-end portion of RAD9p are essential for binding HUSlp. However, the intact HUS lp protein is required for participation in all of the physical interactions observed thus far. Interestingly, we demonstrated that the carboxyl-terminal region of RAD9p is important for binding checkpoint control proteins HUS lp and RADlp, but amino acids near the N-terminal are sufficient to interact with the anti-apoptotic proteins Bcl-2 and Bcl-x, (Komatsu *et* al., 2000), suggesting that RAD9p links and coordinates the cell cycle delay and programmed cell death responses to radiation exposure. In addition, since we found that *HUS1* is expressed at high levels in the testis, just like *RAD1* (Parker et al., 1998a) and *RAD9* (Kevin Hopkins and HBL, unpublished data), and *MRAD1* was already found to participate in a meiotic

checkpoint (Freire *et al.*, 1998), these results suggest a role for the HUS1p-RAD1p-RAD9p complex in this checkpoint process as well. The results of this study are discussed in the context of the potential roles of HUS lp, RAD1p and RAD9p in the response of cells to DNA damage or incomplete DNA replication.

MATERIALS AND METHODS

Bacterial strains and manipulations. *E. coli* strain DH5α was used as a host for plasmid amplification. YT liquid medium (0.5% yeast extract, 0.8% Bacto Tryptone, 0.5% NaCl) or YT agar plates (YT liquid with 1.5% agar) were used to grow bacteria. YT medium with ampicillin (final concentration of 50 μg/ml) was used to select cells containing plasmids with the ampicillin resistance gene. Standard procedures were used to introduce plasmid DNA into *E. coli* (Ausubel *et al.*, 1997).

Yeast two-hybrid analysis. The matchmaker LexA two-hybrid system from Clontech (Palo Alto, CA) was used to screen a library of plasmids encoding proteins that potentially interact with HUSlp. *HUS1* cDNA was amplified by PCR using plasmid ATCC154123 (ATCC; Manassas, VA) as a template, digested with *Bam*HI and *Nco*I, and ligated into the *Bam*HI and *Nco*I sites of pLexA. This generates a "bait" plasmid containing a fusion between HUS1p and the 3'-end of the LexA DNA-binding domain. The library used for screening contained cDNA inserts, originating from RNA within human testis, that were fused to the 3' end of the B42 activation domain in pB42AD (Clontech, Palo Alto, CA). In this system, the reporter genes *LEU2* and *lacZ* were used for detection of protein-protein interactions. Expression of B42AD-fused genes is under control of the *GAL1* promoter that can be suppressed in cells grown on medium containing glucose and devoid of galactose, but induced on medium with galactose and raffinose. Host *S. cerevisiae* EGY48 cells already containing pLexA*HUS1* and p8op-lacZ were transformed with pB42AD library DNA by following the supplier's procedure, and selected for retention of the two original

plasmids and one library plasmid on SD medium (0.67% Yeast nitrogen base, 2.0% agar for solid medium when appropriate; Clontech Yeast Protocols Handbook) devoid of histidine, tryptophan and uracil, and containing glucose as the sole carbon source. About 1 x 10^7 colonies were collected, mixed, and plated on the same medium except also without leucine and containing galactose and raffinose, as well as X-gal. Plates were incubated at 30^oC for 5 days. Blue yeast colonies were randomly picked for further analyses to confirm that two-hybrid interactions were occurring and to determine the DNA sequence of the library plasmid inserts within positive yeast transformants.

A two-hybrid quantitative assay using o-Nitrophenyl-P-D-Galactopyranoside (ONPG) was performed as described by Clontech (Palo Alto, CA), but with a single modification involving the growth of cells that improved sensitivity and reproducibility. Single colonies to be tested were grown overnight in SD liquid medium with glucose but devoid of histidine, tryptophan and uracil. After washing twice, diluted cells (final concentration of $1x10^6$/ml) were incubated again overnight in SD medium with galactose and raffinose but lacking histidine, tryptophan and uracil. Cells were then rediluted to OD, = 0.2 in the same type of medium and incubated shaking at 30^oC for 5 to 6 hrs so they reached OD_{600} = 0.3 to 0.8 before proceeding with the standard assay. D-galactosidase units were calculated as 1,000 x $OD_{420}/(t \times V \times OD_{600})$. Alternatively, SD agar medium with galactose, raffinose and X-gal but lacking histidine, tryptophan, leucine and uracil was also used to analyze qualitatively protein-protein interactions by comparing the blue color change and growth of yeast transformants streaked on the agar plates and incubated at 30^oC for 12 hrs to 2 days.

In order to make plasmid constructs for two-hybrid screening and analysis, *HUS1, RAD1* and *RAD9* open reading frames or chosen fragments were synthesized by using the Advantage 2 PCR and companion procedure (Clontech, Palo Alto, CA). The reactions were performed with the primer pairs listed in Table 1, in conjunction with cDNA templates for the three genes of interest [i.e., *HUS1*: ATCC154123; *RAD1*: cDNA synthesized first from normal human RNA provided by Dr. Debra Wolgemuth (Columbia University, New York, NY); and *RAD9* in pART1, Lieberman et *al.*, 1996]. Amplified full-length or partial open reading frame DNA products were cut with appropriate restriction enzymes listed in Table 1, and inserted into corresponding restriction sites

either in pB42AD or pLexA. The DNA sequences of all cDNA inserts were determined and analyzed by standard procedures (Sanger *et* al., 1977) to verify that they were correct before proceeding.

Coimmunoprecipitation. Two vectors, pCDNA3-6HA (a gift from Dr. Yuzhu Zhang (Fox Chase Cancer Institute, Philadelphia, PA) and pFLAG-CMV-2 (Sigma, St Louis, MO), were used to construct plasmids capable of expressing *HUS1, RAD1*, *RAD9* and *EGFP* in human cells. pCDNA3-6HA contains 6 consecutive HA tags and pFLAG-CMV-2 bears a single FLAG tag. To make pFLAG-CMV2-*RAD1,* the open reading frame of the corresponding cDNA was amplified by PCR using pB42AD-*RAD1* (see Table 1) as template in conjunction with primers 5'-CCCAAGCTTCCCCTTCTGACCCAACAGATC-3' and 5'-CGGGATCCCTATGAC TGCAGAATAATTITATTAATAAC-3'. The amplified DNA was subcloned into the *Hin*dIII *Bam*HI sites of pFLAG-CMV-2, fusing the FLAG tag to the amino terminus of the protein coding sequence. The DNA sequence was determined to confirm that no mistakes were introduced into the gene during the cloning process. pFLAG-CMV-2-*RAD9* was a gift from Mr. Wei Zheng (Columbia University, New York, NY). The other expression plasmids were prepared by releasing cDNAs from different vectors and ligating to the corresponding sites in pFLAG-CMV-2 or pCDNA3-6HA (see Table 2).

Human kidney 293T cells (kindly provided by Dr. Takaaki Sato (Columbia University, New York, NY) served as hosts for plasmid transfections and expression. Lipofectamine plus for the transformation reaction was purchased from Gibco BRL (Grand Island, New York, NY). Cells were grown to 50-80% confluence, and then transfected with 10 μg plasmid DNA following procedures described by Gibco BRL. After 24 hrs incubation at 37°C, transfected cells were lysed in 1 ml ice-cold RIPA buffer (150 mM in NaCl, 1% NP-40, 0.5% DOC, 0.1% SDS, 50 mM tris, pH7.5) containing 30 μg/ml of the protease inhibitor PMSF. Lysed cells were spun at 14,000 rpm in a microcentrifuge for 10-15 min. The supematant was precleared by incubating at 4°C and continuously mixing on a spinning wheel with 20 ul protein A beads for 40 min. The supernatant

was collected after microcentrifuging for 2 min at 14,000 rpm, and immunoprecipitated with either 10 μl HA F-7 affinity beads (Santa Cruz Biotechnology, Inc, Santa Cruz, CA) or 30 μl FLAG M2 affinity beads (Sigma, St Louis, MO) for either 4 hrs or overnight at 4°C. After washing the beads 5 times, 20 or 30 μl of protein lysis buffer were added to the HA or FLAG beads, respectively. Then, the beads were boiled for 5 min. Twenty μl of HA and 5 μl of FLAG precipitated samples were loaded into an SDS PAGE gel, fractionated, and immunoblotted with F-7 anti-HA antibodies (Santa Cruz Technology, Inc, Santa Cruz, CA) or F-3 165 anti-FLAG antibodies (Sigma, St. Louis, MO). Alkaline phosphatase conjugated secondary anti-mouse IgG was used to detect HA-HUS 1p or FLAG-HUS lp by standard western analysis procedures (Harlow and Lane, 1988).

Northern blot analysis. Human multiple tissue northern blots were obtained commercially (Clontech, Palo Alto, CA). Blots were first probed with ^{32}P-labeled *HUS1* cDNA following the procedures described by the vendor. After exposing X-ray film, the radioactive probe was stripped off the blots by rinsing in 0.5% SDS at 90°C to 100°C for 10 min. Radiolabled β-actin cDNA, supplied unlabeled by the vendor, was then used to reprobe blots before another film was exposed.

RESULTS

HUS1 cDNA ***isolation and*** *tissue-specific* ***expression***

An advanced BLAST search of the GenBank dbest data base for sequences homologous to ***S. pombe*** *hus1* identified 12 human cDNAs. Four of these cDNAs were acquired from ATCC (Manassas, VA), and their entire DNA sequence was determined. One of these cDNAs (accession no. AA353895), isolated from a human Jurkat T-cell library, spanned 2.1 kbp and contained a complete 843 bp open reading frame, from bp 61 through 903. The entire DNA sequence was submitted to GenBank and assigned accession no. AF110393. Dean et al. (1998) have independently cloned a similar *HUS1* cDNA (accession no. G41778) which was the identical

length but differed from the one described in this report by 5 bps in the untranslated regions and 1 bp in the open reading frame. However, they both encode the same amino acid sequence. A *HUS1* cDNA open reading frame sequence (accession no. Y16893) was also submitted to GenBank by Kostrub *et* al. (1998), and this sequence is identical to the open reading frame of *HUS1* reported here.

Northern blot analysis was performed to determine whether *HUS1* expression is limited to a specific set of human tissues. As indicated in Fig. 1, *HUS1* mRNA was detected in all 16 human tissues examined. However, the level varied in a tissue-dependent manner, and the highest was observed in testis. *HUS1* mRNA was the least abundant in brain and lung. Three major species of *HUS1* mRNA (approximately 1.3 kb, 2.6 kb and 11 kb in length) were found by this analysis. A low abundance mRNA, 3.2 kb long, also appeared in most tissues but not in skeletal muscle. The two *HUS1* cDNAs (accession nos. AF110393 and G41778), independently cloned by us and Dean ***et*** al. (1998), are 2.1 kb long, and were likely to have been derived from the 2.6 kb mRNA detected on the northern blot. Using the cDNA in this report as a query sequence to again search the human est database, ten *HUS1* cDNA fragments, cloned by employing poly(T) as one of the two primers and sequenced from the poly(T) end, were identified. Interestingly, the 3'-end regions terminated between nucleotide 1065 and 1100 of the cDNA described in this paper. These fragments could be derived from the 1.3 kb *HUS1* mRNA, and might represent alternatively spliced message or artifacts generated during synthesis and cloning.

HUS1p, RAD1p ***and*** *RAD9p* ***form a complex more complicated than a simple heterotrimer***

The pLexA-based matchmaker two-hybrid system from Clontech was used to screen for genes that encode proteins capable of interacting with HUS lp. A fragment of *HUS1* containing the entire open reading frame was inserted into pLexA, and then introduced into ***S. cerevisiae*** EGY48 bearing a human testis cDNA library constructed in pB42AD. A total of 142 yeast colonies capable of growing on medium devoid of leucine and demonstrating ß-galactosidase activity were

randomly selected for further study. Library plasmids were retrieved from these positive colonies, and categorized into 27 groups, based on insert size and *Hae*III enzyme digestion pattern. Partial DNA sequence analysis of two clones from each group indicated that the plasmids represented 20 different library inserts. One out of the 20 groups of inserts contained an open reading frame corresponding to the first 160 of the 280 amino acids of RAD1p protein. Since *S. pombe* huslp and radlp were previously found to interact with each other in a rad9p-dependent manner (Kostrub et al., 1998), the focus of this report has been placed on a detailed analysis of the interaction of the human versions of these gene products, namely HUSlp, RAD1p and RAD9p. The other 19 groups of genes encoding proteins that can interact with HUS lp are currently under investigation.

Two recent reports indicate that HUS lp, RAD 1p and RAD9p can be co-immunoprecipitated (Volkmer and Karnitz, 1999; St. Onge *et* al., 1999). Furthermore, two-hybrid studies by St. Onge *et* al. (1999) also demonstrated that RAD9p and HUSlp, as well as HUSlp and RADlp fusion proteins can bind (St. Onge *et* al., 1999). We have extended these findings by using a different, modified pLexA-based yeast two-hybrid method. As shown Fig. 2A, 2B and 2C, we have detected and quantitated interactions between LexA-HUS lp and AD-HUS1p, LexA(or AD)-HUS1p and AD(or LexA)-RAD1p, as well as between LexA-RAD9p and AD-HUSlp. In addition, using the standard LexA system protocol, no significant interaction between RAD9p and RADlp was observed (data not shown here). The interaction between LexA-HUS1p and AD-HUSlp suggests that there are at least two HUS lp molecules in the HUS1p-RAD1p-RAD9p complex. The interaction between LexA-HUS lp and AD-RADlp was 10 times stronger than that between LexA-RAD1p and AD-HUS1p, and was comparable to the interaction between p53 and SV40 large T (Fig. 2B). These results indicate that fusion orientation is important for this type of analyses. The significance of the nature of the fusion is also applicable to the detection of binding between RAD9p and HUS lp. Only LexA-RAD9 and AD-HUS 1p formed a detectable two-hybrid interaction, not LexA-HUS lp and AD-RAD9p.

Interestingly, all the yeast colonies bearing pB42AD-*RAD1* grew significantly slower than other yeast in liquid SD galactose medium, which induces transcription of genes fused to the

transcription activation domain in this plasmid. Cells containing pB42AD-*RAD1* also grew very slowly as streaks on SD agar galactose plates so that a thin layer of yeast barely converted X-gal into a detectable blue color (sign of a positive two-hybrid interaction). This was especially true when weak two-hybrid interactions were examined. When cells bearing pLexA-*RAD9* and pB42AD-*RAD1* were streaked on agar plates containing galactose as well as X-gal, and incubated for 24 hrs, these cells became slightly blue compared to white negative control cells. However, a longer incubation time of 2 days did not significantly enhance the differences in both color and number of cells, but in fact nearly obliterated the slight differences between the experimental and negative control cells. In addition, western blot analysis revealed that expression of AD-*RAD1* suppresses the synthesis of LexA-RAD9p (data not shown). To avoid the effect of this growth inhibition on cells and its impact on the two-hybrid interaction test, cells bearing pLexA-*RAD9* and pB42AD-*RAD1* were initially grown on agar plates containing glucose. This allows cells to grow, constitutively express LexA-*RAD9*, and accumulate pB42AD-*RAD1* plasmids without the synthesis of AD-RAD1p. Subsequently, a significant number of these well-grown fresh cells were streaked onto agar plates containing X-gal and galactose to induce pB42AD-*RAD1* expression. In this way, a sufficient number of cells would then produce AD-RAD1p protein molecules potentially capable of interacting with LexA-RAD9p, producing ß-galactosidase, and thus converting X-gal into its visible blue product, before adversely affecting growth. Using this strategy, in contrast to the results reported by St. Onge *et al.* (1999), we found a two-hybrid interaction between LexA-RAD9p and AD-RADlp was detected 12 hrs after yeast cells were streaked on the agar medium (see Fig. 3).

To confirm our two-hybrid results indicating that at least two molecules of HUS lp can bind to each other, we performed coimmunoprecipitation experiments. As indicated in Fig. 4, when human 293T kidney cells synthesize HUS 1p tagged with 6HA or FLAG, antibodies against each tag are capable of immunoprecipitating both forms of the protein. When cells received a plasmid expressing only one of the tagged versions of HUS1p, and also an insertless plasmid

corresponding to the second tag, antibodies against the second tag did not mediate coimmunoprecipitation. These results indicate that at least two HUS lp molecules can interact.

Although neither RAD9p nor RADlp homodimerize when examined by the two-hybrid system (data not shown), their self-association was tested by coimmunoprecipitation methodolologies. As indicated in Fig. 5, 293T cells simultaneously synthesizing RAD9p tagged with FLAG or 6HA were examined. When extracts of those cells were immunoprecipitated with anti-FLAG antibodies, and examined on a western blot, we found that anti-HA antibodies could detect HA-RAD9 (Fig. 5, lane 1). These results indicate that at least two molecules of RAD9 can associate with each other. However, because their interaction could not be detected by use of a two-hybrid system, this result suggests that at least two RAD9p molecules do not bind to each other directly but are part of the same large complex of proteins. As indicated in lane 2 of Fig. 5, similar results were also obtained for RADlp. To confirm the previously described two-hybrid results demonstrating that RAD9p and RADlp can bind, a similar coimmunoprecipitation strategy was pursued. Human 293T cells were transfected with plasmids capable of expressing FLAG-tagged ***RAD9*** and 6HA-tagged *RAD1*. After cell extracts were prepared and treated with anti-FLAG antibodies, western analysis using anti-HA antibodies as a probe could detect HA-RADlp in the immunoprecipitant (Fig. 5, lane 3). These results are consistent with our two-hybrid studies indicating that RAD9p and RADlp interact. Anti-FLAG antibodies could not immunoprecipitate HA-RAD9p (Fig. 5, lane 4) or HA-RADlp (Fig. 5, lane 6) when cells were not engineered to synthesize FLAG-tagged proteins.

RADlp and RAD9p binding-domain mapping

Two-hybrid analysis with truncated genes was used to map the regions of HUS lp, RADlp and RAD9p important for the interactions previously detected with the intact versions of the proteins. As indicated in Fig. 6, the region of RADlp from the N-terminus through amino acid

residue 140 is essential and sufficient for interacting with HUSlp. However, the interaction between the RADlp N- 160 peptide and HUS lp is more than seven times stronger than that of the smaller RADlp N- 140 peptide with HUS lp (537 versus 70 units of B-galactosidase), and is comparable to the interaction between the full length RADlp and HUS lp (data not shown). These results suggest that the 20 amino acid region from residue 140 through 160 of RADlp plays an important but not the only role in mediating the interaction between RADlp and HUSlp. Interestingly, as also illustrated in Fig. 6, two fragments of RADlp, the N-terminus through amino acid 194, and residue 195 through the C-terminus can interact with RAD9p. Furthermore, it is likely that the important region of the N-terminal through residue 194 portion of RAD 1p is between amino acids 16 1 and 194 since a fragment containing just the N-terminal through residue 160 cannot bind RAD9p. Therefore, the ability of RAD9p to bind two nonoverlapping fragments of RADlp suggests that the latter protein interacts with the former through more than one site. A comparison of these two regions of RADlp revealed that they contain a highly related group of five amino acids. Residues 163 through 167 are LREAF, and 209 through 213 are LMEAF. Studies are underway to test whether these are the key sites of RADlp that can bind RAD9p.

Figure 7 illustrates the results of a study designed to localize regions of RAD9p important for binding HUS lp and RADlp. As indicated, amino acids 13 1 through the C-terminus of RAD9p are sufficient for binding both RADlp and HUSlp. Although amino acids 261 through the C-terminus are essential for these binding reactions to occur, but it cannot be determined from the data whether this region of RAD9p is sufficient for mediating the protein-protein interactions. When this fragment is ligated into pLexA and paired with pB42AD devoid of an insert, a false positive two-hybrid result is obtained. However, coimmunoprecipitation experiments show that this peptide alone does not have the ability to interact with RADlp and HUSlp (data not shown). Nevertheless, although the first 131 amino acids of RAD9p are not needed for binding the checkpoint control proteins RADlp and HUS lp, residues 16 through 30 correspond to a BH3-like domain capable of interacting with the anti-apoptotic proteins Bcl-2 and Bcl-x_L (Komatsu et al., manuscript submitted). Furthermore, this region is critical for the ability of RAD9p to promote apoptosis. Therefore, these

results suggest that RAD9p has two functional domains, one participating in cell cycle checkpoint control and the other in programmed cell death.

Figure 8 illustrates the results of a similar two-hybrid strategy to map regions of HUS1p important for binding another molecule of HUS lp, RAD 1p or RAD9p. None of the HUS lp fragments made demonstrated binding activity. This was true for binding HUSlp, RAD1p or RAD9p. Only the intact form of HUS lp was positive in this assay. Furthermore, the same results were obtained when pB42AD and pLexA were switched for all two-hybrid plasmid pairs listed in Fig. 8. Since the HUSlp protein fragments can be readily detected in yeast cell-free extracts by western analysis (data not shown), protein instability is not responsible for the negative two-hybrid results. A more likely explanation is that all regions of HUS lp are needed to form a unique tertiary structure essential for interacting with other proteins.

DISCUSSION

A human cDNA encoding a protein bearing significant homology to the product of the *S. pombe hus1* checkpoint control gene has been cloned. The open reading frame is identical to the entire sequence (accession no. Y16893) submitted to Genbank by Kostrub et al. (1998), but is one base different from the open reading frame of the cDNA isolated by Dean *et al.* (1998). In addition, the cDNA in this report and the sequence published by Dean *et al.* (1998) differ by several bps in their untranslated regions. Nevertheless, all three *HUS1* open reading frames encode the identical 280 amino acid long, 3 1.67 kDa protein that is 30% identical and 57% similar to the *S. pombe hus1* gene product. Northern analysis reveals that *HUS1* is expressed in all sixteen tissues examined, but levels vary in a tissue-dependent manner. *HUS1* mRNA is most abundant in testis where *RAD1* and *RAD9* were previously found to be expressed at high levels (Freire *et al.,* 1998; Parker *et al.,* 1998a; Kevin Hopkins and HBL, unpublished data). Since RAD1p may function in a meiotic checkpoint (Freire *et al.,* 1998) and it physically interacts with HUSlp and RAD9p (Volkmer and

Karnitz, 1999; St. Onge et al., 1999; this study), the results suggest that the multi-protein complex may regulate this process as a unit. However, the activity of the complex in meiotic checkpoint control remains to be established directly.

Previous studies by Kostrub and coworkers (1998) indicate that S. *pombe* huslp and radlp checkpoint control proteins physically interact in a rad9p-dependent manner. Furthermore, they found that bleomycin can induce phosphorylation of huslp. These results suggest that the three proteins form a specific complex in fission yeast that mediates DNA damage induced cell cycle checkpoint control. Subsequently, Volkmer and Karnitz (1999) showed by coimmunoprecipitation that human homologues of these three proteins associate in a complex, and that RAD9p, in particular, is highly modified in response to DNA damage induced by high doses of ionizing radiation. St. Onge et *al.* (1999) also showed that RAD9p can physically associate with HUS lp and RAD1p, but in addition provided evidence using two-hybrid methodologies that the latter two proteins likely interact directly, as described for the equivalent proteins in S. *pombe.* These investigators also demonstrated that RAD9p was alternatively phosphorylated in tissue culture cells never deliberately exposed to DNA damaging agents, and we observed the same phenomenon. However, endogenous damage or replication intermediates cannot be ruled out as the cause of this inherent complicated RAD9p phosphorylation pattern observed. The sizes of the modified RAD9 proteins detected are unique for each study. These alternative forms of the protein may be due to differences in the processing machinery of the cells used as hosts, or the examination of endogenous versus ectopically expressed *RAD9*. Nevertheless, the conclusion that RAD9p is post-translationally modified, at least via phosphorylation events, has been observed by all groups of investigators.

As stated previously, two other laboratories reported that HUS1p, RADlp and RAD9p form a complex in immunoprecipitates (Volkmer and Kamitz, 1999; St. Onge *et al.,* 1999). Two-hybrid analysis also showed, qualitatively, binding between BD-RAD9p and AD-HUS1p, as well as between BD-HUS 1p and AD-RADlp (St. Onge *et* al., 1999). However, reversing the above pairing orientations, i.e. between BD-HUS lp and AD-RAD9p, as well as between BD-RAD1p and

AD-HUS Ip, gave negative results. In addition, St. Onge et al. (1999) could not demonstrate a two-hybrid interaction between RAD9p and RADlp. The current report makes use of a different two-hybrid system, as well as coimmunoprecipitation to analyze quantitatively and in more detail the physical interactions among these human checkpoint control proteins. Our results extend previous findings and indicate that this complex is more complicated than a simple heterotrimer. In addition, our results begin to define some of the critical interactions likely to participate in this multi-protein complex.

Using the LexA-based two-hybrid system, as opposed to that based on GAL4 employed by St. Onge et ***al.*** (1999), we found that not only do HUS lp and RADlp, as well as HUS lp and RAD9p interact, but RAD9p also binds RADlp. Furthermore, analyses of truncated versions of these proteins revealed that HUSlp must be intact to demonstrate binding, but specific fragments of RADlp and RAD9p are sufficient for detection of two-hybrid interactions. The amino terminal region of RADlp binds HUS lp, but the carboxyl-terminal region of the protein interacts with RAD9p. Furthermore, we found that the carboxyl-terminal two thirds of RAD9p is sufficient to interact with HUSlp or RADlp. Previous studies have indicated that a BH3-like domain between amino acids 16 and 30 of RAD9p interacts with the anti-apoptotic proteins Bcl-2 and Bcl-x_L, and is sufficient to act as a pro-apoptotic element (Komatsu et ***al.,*** 2000). Since the carboxyl-portion of this protein is important for binding HUSlp and RADlp, the results strongly suggest that RAD9p has two functional domains. The amino terminal region plays a role in apoptosis, whereas the carboxyl-end amino acids mediate cell cycle checkpoint control. Interestingly, the C-terminal end of RAD9p is phosphoryiated (unpublished data), and thus may be important primarily for the cell cycle checkpoint function of the protein. These results suggest that RAD9p may link and coordinate these two important processes in response to DNA damage. Cells may undergo a delay in progression through the cell cycle or initiate programmed cell death depending at least in part on the set of proteins bound to RAD9p.

Coimmunoprecipitation and two-hybrid tests presented in this report indicate that a minimum of two HUSlp molecules can interact with each other. Furthermore, although RADlp-

RADlp and RAD9p-RAD9p interactions could not be demonstrated by two-hybrid studies, alternatively tagged RADlp and RAD9p proteins coimmunoprecipitated from human cell extracts. These results suggest that RAD1p-RAD1p or RAD9p-RAD9p interactions are not direct but that these molecules are associated indirectly through binding to a protein complex acting as a bridge. Perhaps the core of the bridge is multiple, linked HUS1 proteins, but other yet to be identified molecules may perform a similar function.

HUS1p, RADlp and RAD9p are likely to function in multiple pathways capable of determining the cellular response to radiation exposure or incomplete DNA replication in humans. Since it has been demonstrated that the human and/or equivalent yeast versions of these genes regulate cell cycle checkpoint control induced by radiation or hydroxyurea, it is likely that this process is governed by the complex containing all three proteins. However, these proteins may individually join other complexes to mediate additional cellular processes. For example, RAD9p may regulate cell cycle checkpoint control through interactions with HUS1p and RADlp, but participate in apoptosis when independently or even simultaneously binding Bcl-2 and Bcl-x, (Komatsu *et al.,* 2000). Understanding the structure, function and coordination of these complexes should provide important insight into mechanisms of cell cycle checkpoint control as well as other cellular responses to damaged DNA.

ACKNOWLEDGMENTS

We thank Mr. Wei Zheng for providing plasmid pFLAG-CMV-2-*RAD9* and also for helpful discussions. This work was supported by grants from the NIH (GM52493) and DOE (DE-FG07-96ER62309). HBL was supported in part by a NIH Research Career Development Award (CA68446).

REFERENCES

Ausubel, F. M., Brent, R., Kingston, R. E., Moore, D. D., Seidman, J. G., Smith, J. A., and Struhl, K. (1997). "Current Protocols in Molecular Biology," John Wiley and Sons, Inc., New York, NY.

Bao, S., Shen, X., Shen, K., Liu, Y., and Wang, S. F. (1998). The mammalian Rad24 homologous to yeast ***Saccharomyces cerevisiae*** Rad24 and ***Schizosaccharomyces pombe*** Rad17 is involved in DNA damage checkpoint. ***Cell Growth*** *Differ.* **9**:961-967.

Cimprich K. A., Shin, T. B., Keith, C. T., and Schreiber, S. L. (1996). cDNA cloning and gene mapping of a candidate human cell cycle checkpoint protein. *Proc. Natl. Acad.* ***Sci. U S*** A. 93:2850-5.

Cliby, W. A., Roberts, C. J., Cimprich, K.A., Stringer, C. M., Lamb, J. R., Schreiber, S. L., and Friend, S. H. (1998) Overexpression of a kinase-inactive ATR protein causes sensitivity to DNA-damaging agents and defects in cell cycle checkpoints. *EMBO* ***J.*** **17:** 159-69.

Dean, F. B., Lian, L., and O'Donnell, M. (1998). cDNA cloning and gene mapping of human homologs for ***Schizosaccharomyces pombe rad17, radl, and husl*** and cloning of homologs from mouse, ***Caenorhabditis elegans,*** and ***Drosophila melanogaster. Genomics*** **54**:424-36.

Freire, R., Murguia, J. R., Tarsounas, M., Lowndes, N. F., Moens, P. B., and Jackson, S. P. (1998). Human and mouse homologs of ***Schizosaccharomyces pombe radl'*** and ***Saccharomyces cerevisiae*** *RAD1* 7: linkage to checkpoint control and mammalian meiosis. Genes ***Dev.*** **12:2560-2573.**

Grifiths, J. F. and Carr, A. M. (1997). DNA Repair in ***Schizosaccharomyces pombe,*** in DNA damage and Repair. In "Vol. 1: DNA Repair in Prokaryotes an Lower Eukaryotes" (J. A. Nickoloff and M. F. Hoestra, Eds.), pp. 449-475, Humana Press Inc., Totowa, NJ.

Harlow, E., and Lane, D. (1988). Antibodies, A Laboratory Manual, Cold Spring Harbor Laboratory Press, Plainview, NY.

Hartwell, L. H., and Kastan, M. B. (1994). Cell cycle control and cancer. Science 266: 1821-1828.

Hartwell, L. H., and Weinert, T. A. (1989). Checkpoints: controls that ensure the order of cell cycle events. Science **246**:629-634.

Komatsu, K., Miyashita, T., Hang, H., Hopkins, K. M., Zheng, W., Cuddeback, S., Yamada, M., Lieberman, H. B., and Wang, H.-G. (2000). Human homologue of *S. pombe* Rad9 interacts with Bcl-2/Bcl-X_L and promotes apoptosis. *Nature Cell Biol. 2: 1-6.*

Kostrub, C. F., Knudson, K., Subramani, S., and Enoch, T. (1998). Huslp, a conserved fission yeast checkpoint protein, interacts with Radlp and is phosphorylated in response to DNA damage. *EMBOJ.* **17:**2055-2066.

Li, L., Peterson, C. A., Kanter-Smoler, G., Wei, Y. F., Ramagli, L. S., Sunnerhagen, P., Siciliano, M. J., and Legerski, R. J. (1999). RAD17, a structural homolog of the *Schizosaccharomyces pombe RAD1* 7 cell cycle checkpoint gene, stimulates p53 accumulation. Oncogene 18: 1689-99.

Lieberman, H.B., Hopkins, K.M., Nass, M., Demetrick, D., and Davey, S. (1996). A human homologue of the *Schizosaccharomyces pombe rad9*$^+$ checkpoint control gene. *Proc. Natl. Acad. Sci. USA* **93:**13890-13895.

Nojima, H. (1997). Cell cycle checkpoints, chromosome stability and the progression of cancer. **Hum. Cell 10:**221-230.

Parker, A. E., Van de Weyer, I., Laus, M. C., Oostveen, I., Yon, J., Verhasselt, P., and Luyten, W. H. (1998a). A human homologue of the *Schizosaccharomyces* ***pombe*** *rad1*$^{+}$ checkpoint gene encodes an exonuclease. ***J Biol Chem. 273: 18332-9.***

Parker, A. E., Van de Weyer, I., Laus, M. C., Verhasselt, P., and Luyten, W. H. (1998b). Identification of a human homologue of the ***Schizosacchuromyces pombe*** *rad17*$^{+}$ checkpoint gene. ***J. Biol. Chem. 273:*** 18340- 18346.

Sanger, F., Nicklen, S., and Coulson, A. R. (1977). DNA sequencing with chain-terminating inhibitors. *Proc. Natl. Acad.* ***Sci. USA*** **74:**5463-5467.

Smith, L., Liu, S. J., Goodrich, L., Jacobson, D., Degnin, C., Bentley, N., Carr, A. M., Flaggs, G., Keegan, K., Hoekstra, M., and Thayer, M. J. (1998). Duplication of ATR inhibits MyoD, induces aneuploidy and eliminates radiation-induced G 1 arrest. ***Nut. Genet.*** **19: 39-46.**

St. Onge, R. P., Udell, C. M., Casselman, R., and Davey, S. (1999). The human G2 checkpoint control protein RAD9 is a nuclear phosphoprotein that forms complexes with RAD1 and HUS1. Mol. ***Biol. Cell*** **10**:1985-1995.

Tibbetts, R. S., Brumbaugh, K. M., Williams, J. M., Sarkaria, J. N., Cliby, W. A., Shieh, S. Y., Taya, Y., Prives, C., and Abraham, R. T. (1999). A role for ATR in the DNA damage-induced phosphorylation of p53. ***Genes Devel.*** **13**:152-157.

Udell, C. M., Lee, S. K., and Davey, S. (1998). *RAD1* and *MRAD1* encode mammalian homologues of the fission yeast *rad1*$^{+}$ cell cycle checkpoint control gene. *Nucl. Acids Res.* **26**:3971-3978.

Volkmer, E. and Kamitz, L. M. (1999). Human homologues of *Schizosaccharomyces pombe* Radl, Husl and Rad9 form a DNA damage-responsive protein complex. *J. Bid. Chem. 274:567-570.*

Wright, J. A., Keegan, K. S., Herendeen, D. R., Bentley, N. J., Carr, A. M., Hoekstra, M. F. and Concannon, P. (1998). Protein kinase mutants of human ATR increase sensitivity to UV and ionizing radiation and abrogate cell cycle checkpoint control. *Proc. Natl. Acad. Sci. U S A 95:* 7445-50.

Table 1. Primers with restriction sites used to amplify open reading frames to construct plasmids for two-hybrid analysis.

Plasmids'	Primers	Restriction Sites
pLexA-*HUS1*	5'-CGGGATCCTCAAGTTTCGGGCCAAGATCGTG-3'	*Bam*HI
	5'-CATGCCATGGCTAGGACAGTGCAGGGATG-3'	*Nco*I
pLexA-*RAD1*	5'-GGAATTCCCCCTTCTGACCCAACAGATCC-3'	EcoRI
	5'-ACTGCCATAACTCGAGTCAAGACTCAGATTCAGGAACTTC-3'	*Xho*I
pB42AD-*HUS1*	5'-GGAATTCAAGTTTCGGGCCAAGATCGTG-3'	EcoRI
	5'-ACGAATTCCTAGGACAGTGCAGGGATG-3'	*Eco*RI
pB42AD-*HUS1*(98-C)	5'-GGAATTCGCCAGGGCTTTGAAAATC-3'	*Eco*RI
	5'-ACGAATTCCTAGGACAGTGCAGGGATG-3'	EcoRI
pB42AD-*HUS1*(188-C)	5'-GGAATTCGGAGAATTGAATTTGAAAATAG-3'	EcoRI
	5'-ACGAATTCCTAGGACAGTGCAGGGATG-3'	EcoRI
pB42AD-*HUS1*(N-97)	5'-GGAATTCAAGTTTCGGGCCAAGATCGTG-3'	EcoRI
	5'-GGAATTCCTAATTCTGGGCAGTCTTCAAG-3'	EcoRI
pB42AD-*HUS1*(N-187)	5'-GGAATT CAAGTTTCGGGCCAAGATCGTG-3'	EcoRI
	5'-GGAATTCCTAATCTAGGTTTGCTTCAATAAC-3'	EcoRI
pB42AD-*RAD1*	5'-GGAATTCCCCC'ITCTGACCCAACAGATCC-3'	EcoRI
	5'-ACTGCCATAACTCGAGTCAAGACTCAGATTCAGGAACTTC-3'	*Xho*I
pB42AD-*RAD1*(51-C)	5'-GGAATTCGTAACAGTGGAAAATGCAAAGTG-3'	EcoRI
	5'-ACTGCCATAACTCGAGTCAAGACTCAGATTCAGGAACTTC-3'	*Xho*I
pB42AD-*RAD1*(51-140)	5'-GGAATTCGTAACAGTGGAAAATGCAAAGTG-3'	EcoRI
	5'-ATTCGGCCGACTCGAGCTCAGGTTCCTGTGTATTG-3'	*Xho*I
pB42AD-*RAD1*(N-194)	5'-GGAATTCCCCCTTCTGACCCAACAGATCC-3'	EcoRI
	5'-ACTGCCATAACTCGAGCTATCCAAAAGTAGATAACCTG-3'	*Xho*I
pB42AD-*RAD1*(N-140)	5'-GGAATTCCCCCTTCTGACCCAACAGATCC-3'	EcoRI
	5'-ATTCGGCCGACTCGAGCTCAGGTTCCTGTGTATTG-3'	*Xho*I
pB42AD-*RAD1*(N-97)	5'-GGAATTCCCCCTTCTGACCCAACAGATCC-3'	EcoRI
	5'-ACTGCCATAACTCGAGCTATCCAAAAATAGATAAACAG-3'	*Xho*I
pB42AD-*RAD9*	5'-TAGGCATCCTCGAGAAGTGCCTGGTCACGGGC-3'	*Xho*I
	5'-AGCTCATTCTCGAGTCAGCCTTCACCCTCACTG-3'	*Xho*I
pLexA-*RAD9*	5'-CGGGATCCTAAAGTGCCTGGTCACGGGC-3'	*Xho*I
	5'-AGCTCATTCTCGAGTCAGCCTTCACCCTCACTG-3'	*Xho*I
pLexA-*RAD9*(N-130)	5'-CGGGATCCTAAAGTGCCTGGTCACGGGC-3'	*Xho*I
	5'-ACTGCCATAACTCGAGCTACTCACAGTCCTGGAAGGACAGG-3'	*Xho*I
pLexA-*RAD9*(N-260)	5'-CGGGATCCTAAAGTGCCTGGTCACGGGC-3'	*Xho*I
	5'-ACTGCCATAACTCGAGCTAAAAGTGGCCGTCCAGCAAAGAG-3'	*Xho*I
pLexA-*RAD9*(131-C)	5'-ACTGCCTCCCCTCGAGTCCCTGCAGGCCGTCTTCGAC-3'	*Xho*I
	5'-AGCTCATTCTCGAGTCAGCCTTCACCCTCACTG-3'	*Xho*I
pLexA-*RAD9*(261-C)	5'-ACTGCCTCCCCTCGAGGTCTTGGCCACACTCTCAGAC-3'	*Xho*I
	5'-AGCTCATTCTCGAGTCAGCCTTCACCCTCACTG-3'	*Xho*I

When indicated, only part of cDNA open reading frames encoding protein fragments were subcloned.

Table 2. Construction of mammalian expression vectors.

Plasmid Constructs		Plasmid Sources of cDNAs	
Plasmid Name	Restriction Sites	Plasmid Name	Restriction Sites
pFLAG-CMV-2-*HUS1*	*Eco*RI	pB42AD-*HUS1*	*Eco*RI
pFLAG-CMV-2-*EGFP*	*Hind*III/*Sal*I	pREP41-*EGFP*	*Hind*III/*Sal*I
pCDNA3-6HA-*HUS1*	*Eco*RI/*Not*I	pLexA-*HUS1*	*Eco*RI/*Not*I
pCDNA3-6HA-*RAD1*	*Eco*RI/*Xho*I	PLexA-*RAD1*	*Eco*RI/*Xho*I
pCDNA3-6HA-*RAD9*	*Xho*I	PLexA- *RAD9*	*Xho*I

FIGURE LEGENDS

Figure 1. Northern blot analysis of *HUS1* mRNA in different human tissues. See Materials and Methods for experimental details.

Figure 2. Two-hybrid interactions between HUS lp and (A) HUS lp, (B) RAD1p, or (C) RAD9p. Panel B in addition illustrates the interaction between p53 and SV40 large T. ß-galactosidase activity produced from *S. cerevisiae* EGY48 cells containing the indicated plasmids are illustrated, and were determined as described in the Materials and Methods section. Presented are the results averaged from three independent experiments. Error bars represent standard deviation.

Figure 3. Two-hybrid interaction between LexA-RAD9p and AD-RAD1p fusion proteins. S. *cerevisiae* EGY48 cells containing pLexA and pB42AD, either devoid of inserts (denoted with a dash) or bearing the genes indicated, were initially grown on SD agar medium with glucose, then streaked onto SD agar with X-gal and galactose instead of glucose (see Materials and Methods, and Results sections for details). Five independent transformants for each two-plasmid pair combination were examined.

Figure. 4 Multiple HUS lp molecules can be coimmunoprecipitated from human cell extracts. pFLAG-CMV-2-*HUS1* and p6HA-*HUS1*, which can express alternatively tagged *HUS1*, were cotransfected into 293T human kidney cells. After incubation for 24 hrs, the supematant from the cell lysate was immunoprecipitated with anti-FLAG or anti-HA antibodies, then probed individually with the same two antibodies, as indicated. Insertless plasmids served as negative controls.

Figure. 5 Coimmunoprecipitation indicates that RADlp and RAD9p can self-associate or form a heteroprotein complex in human cells. Human 293T cells were transfected with pairs of plasmids containing the FLAG (FL) or 6HA (HA) tagged fusion genes indicated, or the latter with a plasmid encoding just the FLAG tag. After 24 hrs, cell extracts were prepared and treated with anti-FLAG antibodies, Immunoprecipitates were then probed with anti-HA antibodies by western analysis.

Figure 6. Two-hybrid analysis to define regions of RAD lp important for binding HUS lp and RAD9p. pB42AD containing either the intact *RAD1* cDNA or truncated versions encoding fragments of the protein, as indicated, were introduced along with pLexA-*HUS1*, pLexA-*RAD9* or the insertless pLexA control vector into S. *cerevisiae* EGY48 cells for two-hybrid analyses. The quantitative two-hybrid test was used to assess interactions between AD-RADlp (intact or fragment versions of the RAD lp) and LexA-HUS lp (see Fig. 2), whereas LexA-RAD9p and AD-RAD1p binding was examined by the two-hybrid spot test (see Fig. 3). The negative control tests using pLexA devoid of an insert were compiled from both spot and quantitation assays. Top figure summarizes two-hybrid test results. Bottom figure illustrates protein binding domains. +, indicates above seven B-galactosidase units, the highest background level obtained for this set of experiments, for the quantitative two-hybrid assay. (In fact, 70 units was the lowest level above background that was scored as a positive interaction), or a visible blue color above background for the qualitative spot test; -, indicates four or lower ß-galactosidase units, for the quantitative two-hybrid assay, or a white streak comparable to background color for the qualitative spot test.

Figure 7. Two-hybrid analysis to define regions of RAD9p important for binding HUS1p and RADlp. pLexA-*RAD9* containing the intact ***RAD9*** cDNA, or truncated versions encoding fragments of the corresponding protein as indicated, were cotransfected with either pB42AD-*HUS1*, pB42AD-*RAD1* or pB42AD vector into S. *cerevisiae* EGY48 cells for two-hybrid analyses.

The qualitative two-hybrid spot test was used for these experiments (see Fig. 3). Top figure summarizes two-hybrid test results. Bottom figure illustrates protein binding domains. +, indicates a visible blue color above background; -, indicates a white streak comparable to background color for the qualitative spot test.

Figure 8. Two-hybrid analysis to define regions of HUS1p important for binding HUS1p, RAD1p and RAD9p. pB42AD containing the intact *HUS1* cDNA, or truncated versions encoding fragments of the corresponding protein as indicated, were cotransfected with pLexA-*HUS1*, pLexA-*RAD1* or pLexA-*RAD9* into *S. cerevisiue* EGY48 cells for two-hybrid analyses. The data were derived from two-hybrid quantitative assays (see Fig. 2). +, indicates above four ß-galactosidase units, the highest background level obtained for this set of experiments, for the quantitative two-hybrid assay. (In fact, 22 units was the lowest level above background that was scored as a positive interaction); -, indicates four or lower ß-galactosidase units, for the quantitative two-hybrid assay.

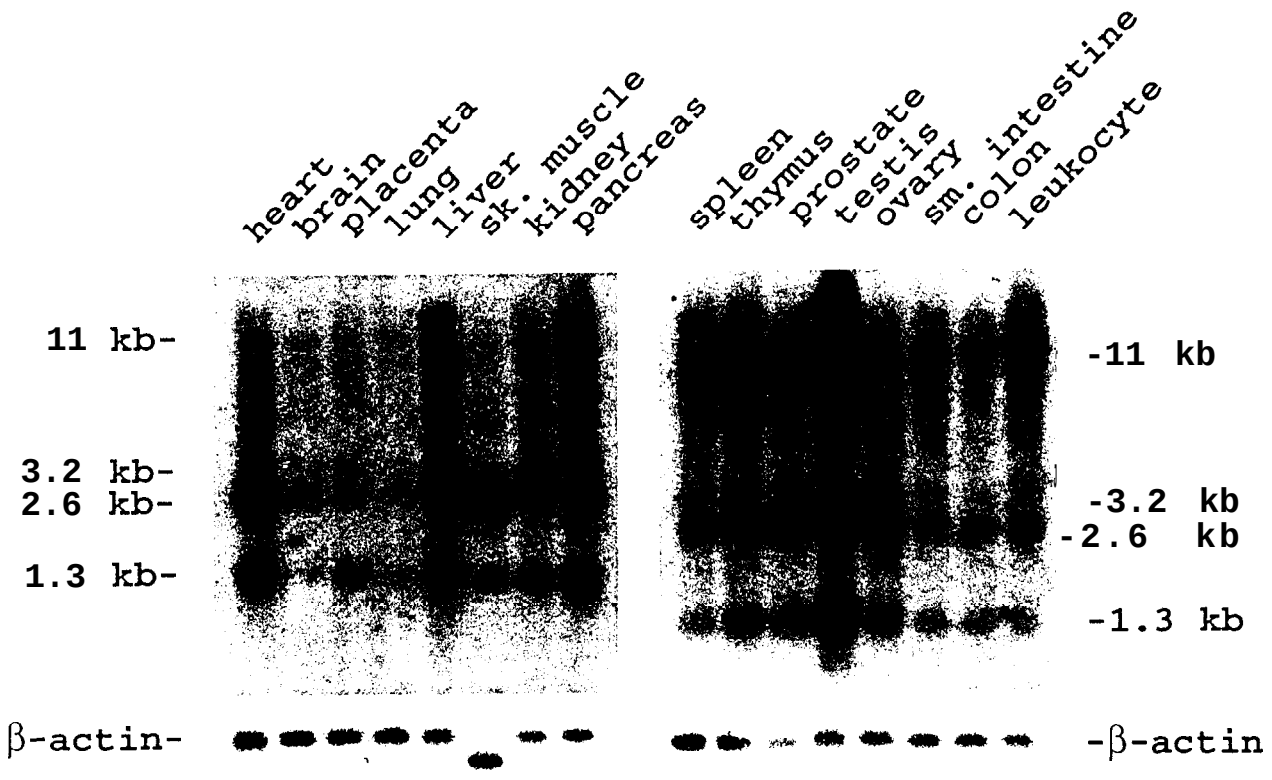
heart
brain
placenta
lung
liver
sk. muscle
kidney
pancreas
spleen
thymus
prostate
testis
ovary
sm. intestine
colon
leukocyte
11 kb-
3.2 kb-
2.6 kb-
1.3 kb-
β-actin-
-11 kb
-3.2 kb
-2.6 kb
-1.3 kb
-β-actin

A
B
C
β-Galactosidase Units
100
80
60
40
20
0
7000
6000
5000
4000
3000
2000
1000
0
100
80
60
40
20
0
pB42AD->
pLexA->
HUS1/HUS1
HUS1/ -
- /HUS1
p53 / T
HUS1/RAD1
RAD1/HUS1
- /RAD1
RAD1/ -
- /HUS1
HUS1/ -
RAD9/HUS1
HUS1/RAD9
RAD9/ -
- /HUS1
HUS1/ -
- /RAD9

2 of 4

pLexA →	*RAD9*	*RAD9*	–	*RAD1*
pB42AD →	*RAD1*	–	*RAD1*	*RAD9*

Fig 3

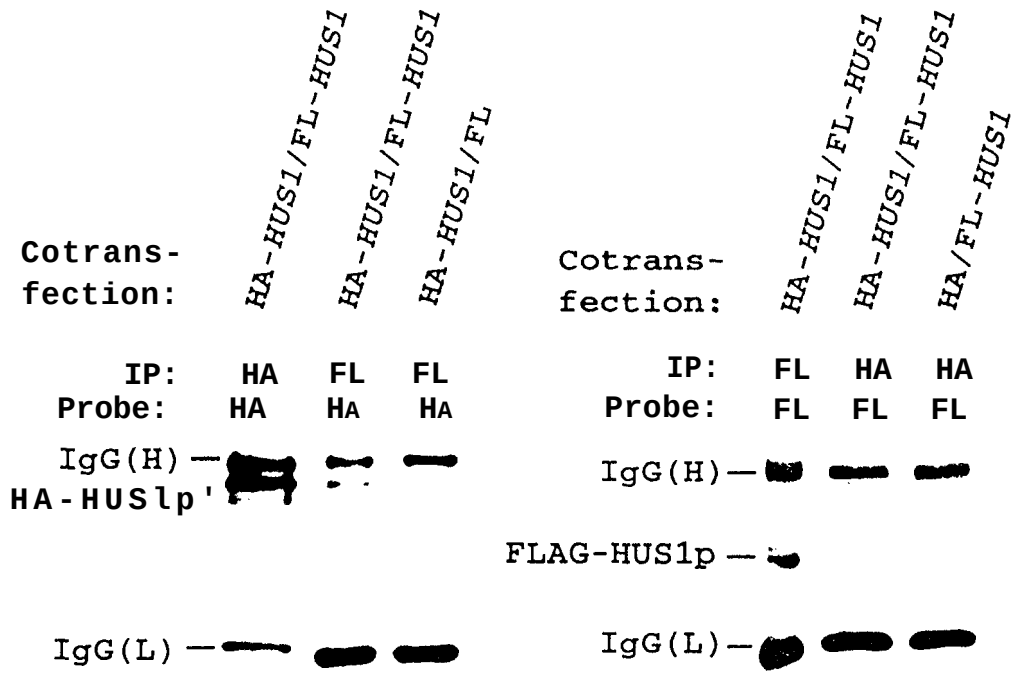
Cotrans-
fection:
HA-HUS1/FL-HUS1
HA-HUS1/FL-HUS1
HA-HUS1/FL
IP: HA FL FL
Probe: HA HA HA
IgG(H)
HA-HUSlp'
IgG(L)
Cotrans-
fection:
HA-HUS1/FL-HUS1
HA-HUS1/FL-HUS1
HA/FL-HUS1
IP: FL HA HA
Probe: FL FL FL
IgG(H)
FLAG-HUS1p
IgG(L)

Fig 4

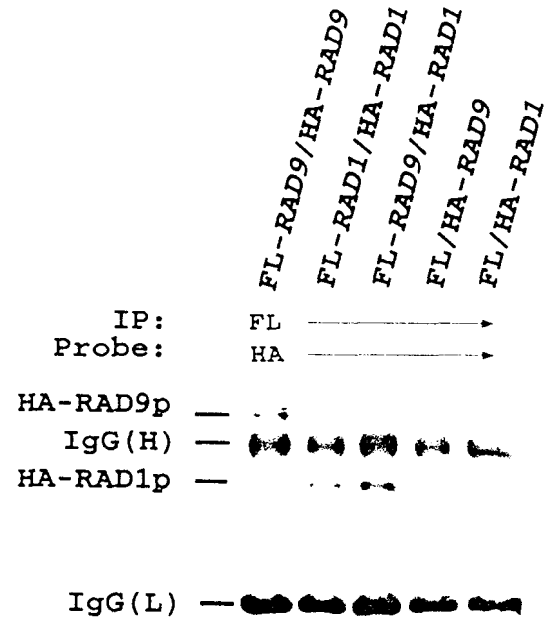
FL-RAD9/HA-RAD9
FL-RAD1/HA-RAD1
FL-RAD9/HA-RAD1
FL/HA-RAD9
FL/HA-RAD1
IP:
Probe:
FL
HA
HA-RAD9p
IgG(H)
HA-RAD1p
IgG(L)

Fig 5

Plasmids Cot ransf ormed			
pB42AD-*RAD1*	pLexA-*HUS1* or	pLexA-*RAD9* or	pLexA
N ▬▬▬▬▬▬▬▬ C (282)	+	+	
N ▬▬▬ 97		-	-
51 ▬▬▬ 140		-	-
N ▬▬▬ 140	+	-	-
N ▬▬▬ *160*	+		-
N ▬▬▬ 194	+	+	-
51 ▬▬▬ C		+	-
98 ▬▬▬ C	-	+	-
195 ▬▬▬ C	-	+	-

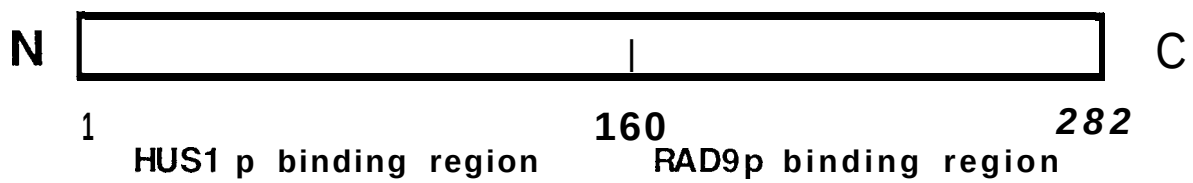

Fig 6

Plasmids Cotransformed

pLexA-*RAD9*	pB42AD-*HUS1*	or	pB42AD-*RAD1*	or	pB42AD
N ——— C (391)	+		+		-
N ——— 130	-		-		-
N ——— 26°	-		-		-
131 ——— C	+		+		-
261 ——— C	+		+		+

BH3-like domain (16-30)

RAD1p & HUS1p binding region

Fig 7

Plasmids	Cot ransf ormed
pB42AD-*HUS1*	pLexA-*HUS1* pLexA-*RAD1* pLexA-*RAD9*
N ▬▬▬